



Tuning the activity of alternative Ru-based initiators for ring-opening metathesis polymerization of norbornene and norbornadiene by the substituent in 4-CH₂R-piperidine



Henrique K. Chaves^a, Camila P. Ferraz^a, Valdemiro P. Carvalho Jr^b,
Benedito S. Lima-Neto^{a,*}

^a Instituto de Química de São Carlos, Universidade de São Paulo, CP 780, CEP 13560-970, São Carlos, SP, Brazil

^b Departamento de Física, Química e Biologia, Faculdade de Ciências e Tecnologia, Universidade Estadual Paulista, CEP 19060-900, Presidente Prudente, SP, Brazil

ARTICLE INFO

Article history:

Received 20 November 2013

Received in revised form 6 January 2014

Accepted 14 January 2014

Available online 24 January 2014

Keywords:

ROMP

Ruthenium

Piperidine

Norbornene

Norbornadiene

ABSTRACT

The novel [RuCl₂(PPh₃)₂(4-CH₂R-pip)] complexes, with R=H (complex **1**), Ph (**2**) or OH (**3**), were synthesized and applied as initiators for ROMP of norbornene (NBE) and norbornadiene (NBD) under different reaction times, temperatures and monomer concentrations. There is a clear difference in the homopolymer yields in the order **1**>**2**>**3** at [monomer]/[Ru] molar ratio of 5000, at 25 °C for 5–60 min. Difference in the yields tends to disappear at 50 °C, with quantitative yields for 15–30 min with any type of initiator. Results from copolymers obtained at RT for 60 min from fixed amounts of NBE with four different amounts of NBD suggest that the type of initiator also affects the reactions, with more insertion of NBD with **1**. The occurrence of cross-linking enhanced as the NBD loading increased, evidenced by decrease in the M_c and increase in the T_g values, besides the influence of the type of initiator.

© 2014 Elsevier B.V. All rights reserved.

1. Introduction

Olefin metathesis (OM) is an efficient accessible synthetic tool for tailoring organic molecules and producing polymers with retention of the olefinic unsaturation in the resulting compounds [1–4].

New approaches using this type of reaction have been continuously tested worldwide [5–7] owing to the development of well-defined transition metal-based initiator complexes. This is a consequence of the recognition that the mechanism of catalytic reaction occurs via metallocarbene species [5–7].

In particular, Ru-based Grubbs-type initiators have been used for various OM applications with very good activity even in the presence of many organic functional groups, with reasonable stability in the presence of air and moisture [5–7]. This behavior can be associated with the chemical nature of the ruthenium ion combined with the presence of appropriate ancillary ligands in the coordination sphere.

The understanding of the types of initiators is very important for planning modifications in the search for quality improvements and the discovery of new starting compounds [1–7]. Besides the importance of carbene moiety to well-defined OM initiators, the

search for novel active catalytic species, which can be readily generated *in situ* at low cost from either organometallic or Werner type initiators, is still a stimulating challenge [8–14]. This could be an alternative for the well-defined Ru-based initiators.

Our research group has developed [RuCl₂(phosphine)_x(amine)_y] type complexes for ring-opening metathesis polymerization (ROMP) and ROM-copolymerization (ROMCP) [15–21]. The electronic combination of π -acceptor phosphine with σ -donor amine is a convenient modular approach to tune the reactivity of such initiators when varying the amine electronic nature, in addition to generating an appropriate steric hindrance balance. These are long-term air-stable complexes because of their phosphine nature and they present high reactivity within few minutes at room temperature. The resulting polymers show moderate PDI values from runs at [monomer]/[Ru] molar ratio of 5000–15,000. It is worth mentioning that this type of compound utilizes cheap friendly ligands, which could be suitable for preparative scale. In particular, successful results were obtained combining PPh₃ with piperidine or 3,5-dimethyl-piperidine [19–21], and this fact was an alert to explore other functionalized piperidines.

Therefore, as part of a continuous interest in the development of alternative initiators for ROMP for preparative scale, this article reports the preparation of [RuCl₂(PPh₃)₂(4-CH₂R-pip)] type complexes, where the R substituent is H (for complex **1**), Ph (for **2**) and OH (for **3**). Ethyldiazoacetate (EDA) was used as the starting source

* Corresponding author. Tel.: +55 16 33739953; fax: +55 16 33739976.

E-mail address: benedito@iqsc.usp.br (B.S. Lima-Neto).

of carbene. The study aims to evaluate how minor changes in the amine ligand can influence the metal reactivity for ROMP of NBE and NBD under different conditions of reaction time, temperature and monomer concentration.

The occurrence of ROMCP with novel initiators was also studied when the reactions were started with a fixed quantity of NBE (5000 equiv./[Ru]) and different amounts of NBD (500, 1000, 1500 and 2000 equiv./[Ru]). Reactions with different NBD loading were performed to evaluate the occurrence of crosslinking in the resulting material and the influence in the thermal-mechanical properties.

2. Experimental

2.1. General remarks

All manipulations were performed under argon or nitrogen atmosphere. HPLC-grade CHCl_3 was used throughout. Other solvents were of analytical grade and were distilled from the appropriate drying agents prior to use. Other commercially available reagents were used without further purification. $\text{RuCl}_3 \cdot x\text{H}_2\text{O}$, norbornene (NBE), norbornadiene (NBD), 4-methylpiperidine (4- CH_3 -pip), 4-benzylpiperidine (4- CH_2Ph -pip), 4-piperidinemethanol (4- $\text{CH}_2(\text{OH})$ -pip), and ethyldiazoacetate (EDA), from Aldrich were used as acquired. The $[\text{RuCl}_2(\text{PPh}_3)_3]$ complex was prepared following the literature and its purity was verified by satisfactory elemental analysis and spectroscopic examination ($^{31}\text{P}\{\text{H}\}$ and ^1H NMR; FTIR) [22–24]. The room temperature (RT) was $24 \pm 1^\circ\text{C}$.

2.2. Synthesis of the $[\text{RuCl}_2(\text{PPh}_3)_2(4\text{-CH}_2\text{R-pip})]$ complexes (**1**, **2** and **3**)

The amine (4- CH_3 -pip, 4- CH_2Ph -pip or 4- $\text{CH}_2(\text{OH})$ -pip; 0.34 mmol) was added to a solution of $[\text{RuCl}_2(\text{PPh}_3)_3]$ (0.26 mmol; 0.25 g) in acetone (40 mL). The resulting dark green solution was stirred for 2 h at RT. A green precipitate was formed, filtered, washed with methanol and ethyl ether, and then dried in vacuum.

Complex **1** ($\text{R}=\text{H}$): 75% yield. Analytical data for $\text{RuCl}_2\text{P}_2\text{NC}_{42}\text{H}_{43}$ are 63.40C, 5.45H, and 1.76% N; found 63.59C, 5.47H, and 1.88% N. FTIR in CsI : 322 cm^{-1} for $\nu(\text{Ru}-\text{Cl})$; 3228 cm^{-1} for $\nu(\text{N}-\text{H})$. $^{31}\text{P}\{\text{H}\}$ NMR in CDCl_3 : 62.7 ppm (s).

Complex **2** ($\text{R}=\text{Ph}$): 58% yield. Analytical data for $\text{RuCl}_2\text{P}_2\text{NC}_{48}\text{H}_{47}$ are 66.13C, 5.43H, and 1.61% N; found 66.41C, 5.37H, and 1.72% N. FTIR in CsI : 320 cm^{-1} for $\nu(\text{Ru}-\text{Cl})$; 3257 cm^{-1} for $\nu(\text{N}-\text{H})$. $^{31}\text{P}\{\text{H}\}$ NMR in CDCl_3 : 62.7 ppm (s).

Complex **3** ($\text{R}=\text{OH}$): 67% yield. Analytical data for $\text{RuCl}_2\text{P}_2\text{NC}_{42}\text{H}_{43}\text{O}$ are 62.15C, 5.34H, and 1.73% N; found 62.19C, 5.26H, and 1.83% N. FTIR in CsI : 323 cm^{-1} for $\nu(\text{Ru}-\text{Cl})$; 3230 cm^{-1} $\nu(\text{N}-\text{H})$. $^{31}\text{P}\{\text{H}\}$ NMR in CDCl_3 : 62.7 ppm (s).

2.3. Polymerization reactions

In a typical ROMP experiment, 1.1 μmol of an initiator (**1**, **2** or **3**) was dissolved in 2 mL of CHCl_3 with an appropriate amount of monomer (NBE or NBD), followed by the addition of EDA. Usually, the solution was gelled in 1–2 min, but the reaction mixture was stirred for an additional period at 25 or 50 $^\circ\text{C}$ in silicon oil bath ($\pm 1^\circ\text{C}$). At RT, methanol (c.a. 5 mL) was added and the polymer was filtered, washed with methanol, and dried in vacuum oven at 27 $^\circ\text{C}$ until a constant weight was achieved. The reported yields are average values from catalytic runs performed at least three times, with maximum 10% error. The isolated polyNBEs were dissolved in 2 mL of CHCl_3 for GPC data.

In a typical ROMCP experiment, an appropriate NBE amount was dissolved in 2 mL of CHCl_3 at RT to result in a $[\text{NBE}]/[\text{Ru}] = 5000$ (means, $[\text{NBE}]_{5000}$): 6.30 mmol in the case of **1**, 5.74 mmol in

the case of **2**, and 6.16 mmol in the case of **3**. Then NBD was added to result in a $[\text{NBD}]/[\text{Ru}] = n$ (means, $[\text{NBD}]_n$): 0.63 mmol (**1**), 0.57 mmol (**2**), and 0.61 mmol (**3**) for $n = 500$; 1.26 mmol (**1**), 1.15 mmol (**2**), and 1.23 mmol (**3**) for $n = 1000$; 1.88 mmol (**1**), 1.72 mmol (**2**), and 1.85 mmol (**3**) for $n = 1500$; and 2.51 mmol (**1**), 2.29 mmol (**2**), and 2.46 mmol (**3**) for $n = 2000$. The polymerization reaction was initiated by adding 1.1 μmol of an initiator (**1**, **2** or **3**), followed by the addition of 2 μL of EDA. After 60 min, methanol (c.a. 5 mL) was added and the precipitated material was filtered, washed with methanol, and dried in vacuum oven at 27 $^\circ\text{C}$ until a constant weight was achieved.

For NMR measurements, the isolated polymers were reprecipitated with methanol from CHCl_3 solutions, and then dissolved in CDCl_3 .

The films for DMA measurements were prepared in Teflon molds (disks of 65 mm) via solution-cast from saturated CHCl_3 solutions.

2.4. Equipment

Elemental analyses were performed in a Perkin-Elmer CHN 2400 in the Elemental Analysis Laboratory at the Institute of Chemistry – USP. ESR measurements from solid sample were carried out at 77 K, using a Bruker ESR 300C apparatus (X-band) equipped with a TE102 cavity and HP 52152A frequency counter. FTIR measurements were performed in CsI pellets on a Bomem FTIR MB 102. The NMR (^1H ; $^{13}\text{C}\{^1\text{H}\}$; $^{31}\text{P}\{^1\text{H}\}$) spectra were obtained in CDCl_3 at $25.0 \pm 0.1^\circ\text{C}$ using Bruker AC-200 and Bruker AVANCE-III spectrometers. The obtained chemical shifts were reported in ppm relative to TMS or 85% H_3PO_4 . SEC analyses were carried out on a Shimadzu Prominence LC system equipped with a LC-20AD pump, a DGU-20A5 degasser, a CBM-20A communication module, a CTO-20A oven at 27 $^\circ\text{C}$, and a RID-10A detector connected to three PL gel columns (5 μm MIXED-C: 30 cm, $\varnothing = 7.5$ mm). Retention time was calibrated with standard monodispersed polystyrene using HPLC-grade CHCl_3 as eluent. PDI is M_w/M_n . The storage modulus (E') and loss tangent ($\tan \delta$) were recorded as a function of the temperature using a Netzsch Instruments DMA 242C, with a heating rate of 3.0 $^\circ\text{C}/\text{min}$, working in the tensile mode at a fixed frequency of 1 Hz. Liquid N_2 was used to cool the sample and provide inert atmosphere for the analyses.

3. Results and discussion

3.1. Synthesis and characterization of the new complexes

The isolated compounds presented CHN elemental analyses in agreement with five-coordinated $[\text{RuCl}_2(\text{PPh}_3)_2(4\text{-CH}_2\text{R-pip})]$ type complex compositions, with $\text{R} = \text{H}$ (complex **1**), Ph (complex **2**), or OH (complex **3**).

Typical amine stretching bands in the FTIR spectra characterized the amines in the coordination metal sphere. The $\nu(\text{N}-\text{H})$ bands were shifted toward lower wavenumbers (3220 – 3260 cm^{-1}) when compared to the $\nu(\text{N}-\text{H})$ bands in the uncoordinated piperidine ligands (c.a. 3280 cm^{-1}), which are consistent with the coordination of the 4- CH_2R -piperidine molecules. The FTIR spectra showed only one $\nu(\text{Ru}-\text{Cl})$ band at c.a. 320 cm^{-1} in each case, suggesting that the two Cl^- ligands are arranged in the *trans* positions, as in $[\text{RuCl}_2(\text{phosphine})_3]$ with phosphine = PPh_3 or PPh_2Bz [19,22–26].

The ^{31}P NMR spectrum in CDCl_3 at 25 $^\circ\text{C}$ showed only one singlet signal at 62.7 ppm in each case, suggesting equivalent phosphine ligands. Correlating this fact with the observations from the FTIR spectra with respect to the Cl^- ligands, the complexes can be arranged in a square pyramidal (SP) type configuration, with the 4- CH_2R -piperidine ligands at the apical positions (Fig. 1). The ESR spectra were silent, suggesting that the complexes are diamagnetic

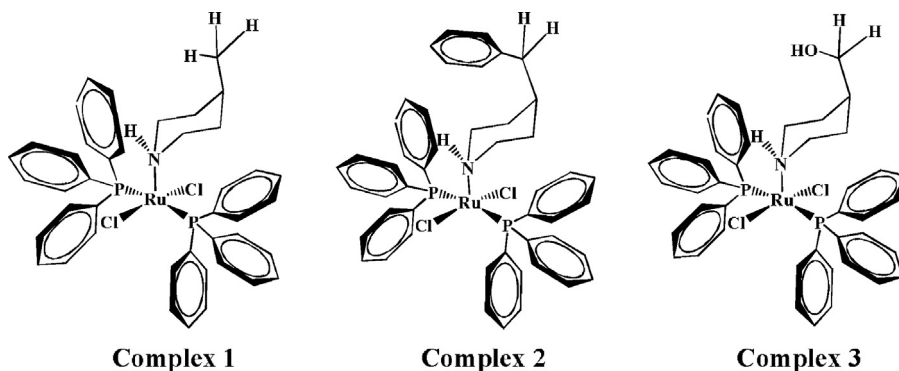


Fig. 1. Illustration of the possible structures of complexes **1** ($R = H$), **2** ($R = Ph$), and **3** ($R = OH$).

in a low spin d⁶ electronic configuration of Ru^{II} complexes, giving support to the SP arrangements [23].

The ³¹P NMR measurements showed the appearance of a signal at 45.0 ppm as a function of time with concomitant disappearance at 62.7 ppm in each case. This fact is associated with the intramolecular geometrical rearrangement to the trigonal bipyramidal (TBP) type configuration (Scheme 1, species II), probably owing to the steric hindrance of PPh₃ in the SP configuration. The PPh₃ ligands are now localized in the axial axis, remaining chemically equivalent, whereas the 4-CH₂R-pip is in the equatorial planes of the complexes. Further, the Cl⁻ ligands remained in the equatorial planes, but with smaller Cl–Ru–Cl angles than those of the SP arrangements [23].

The signal at 45.0 ppm was not observed when the complexes were dissolved in PPh₃ or amine solutions. Similar behavior was also observed in previous studies on PPh₃–Ru–amine complexes [15,19,20].

No other signal was observed in the ³¹P NMR spectra for 12 h. This fact indicates the absence of dissociated PPh₃ ligands or dimer complexes in the solution, unlike the case of [RuCl₂(PPh₃)₃] upon dissolution in CHCl₃ at RT [22–24].

It is interesting to emphasize that the variations in both Ru–Cl stretches and ³¹P-NMR signals were not significant when changing the R substituent groups in the 4-CH₂R-piperidine complexes. At a first moment, this can induce the thought that the R substituents are innocent.

3.2. Synthesis of polymers from NBE

The yields showed favorable dependence on the volume of EDA up to 2 μL ([EDA]/[Ru] ~ 20), with a tendency of decreasing for larger volumes (Fig. 2). The excess of EDA ([EDA]/[Ru] ~ 20) can inhibit the propagation reaction owing to a competitive coordination of EDA moiety to the catalytically active species or to the occurrence of secondary reactions, as reported in other studies [12,26–28]. This implies uncontrolled reactions, resulting in polymers with high PDI values (Fig. 2; Table S1). It is worth noting the same curve profiles in Fig. 2 when changing the initiator. However, the difference in results in each case is clear. The best yields and PDIs (from c.a. 2.1 to 2.4) were obtained with **1**; whereas with **3**, the yields dropped to nearly zero and the PDIs increased significantly (from c.a. 1.8 to 6.6). Considering the good results with 2 μL of EDA, this volume was selected for the next studies.

In experiments increasing the reaction time at 25 °C (Fig. 3), the yields increased up to 85% for 60 min when the initiator was changed, following saturation curve profiles in the order **1** > **2** > **3**. At 50 °C, the yields only diverged for 5 min of reaction; quantitative yields were obtained for 5 min with **1** and for 15 min with **2** and **3**.

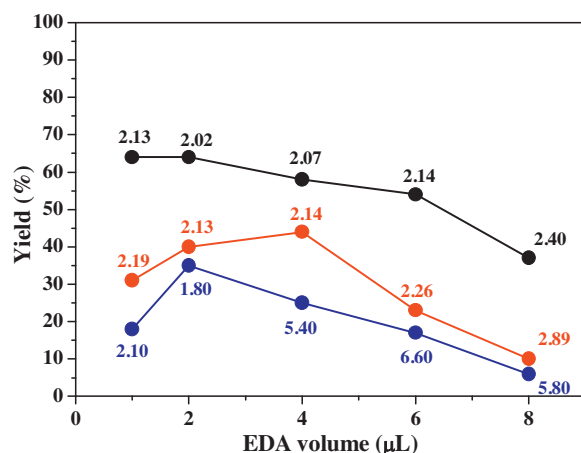


Fig. 2. Dependence of yield on the [EDA]/[Ru] molar ratio for ROMP of NBE with **1** (●), **2** (●), and **3** (●); [NBE]/[Ru] = 5000 with 1.1 μmol of initiator in CHCl₃ at 25 °C for 5 min. The numbers are the PDI values for each run.

Fig. 4 shows that quite quantitative yields were obtained for [NBE]/[Ru] molar ratios in the range of 1000–5000 at 50 °C for 30 min. At 25 °C, c.a. 30% improvement was observed with **2** and **3** when the molar ratios increased from 1000 to 5000, whereas the yields practically doubled when using **1** (from c.a. 35 to 65%). In this way, the reactions are monomer dependent and the yields appear to be susceptible to the initiator.

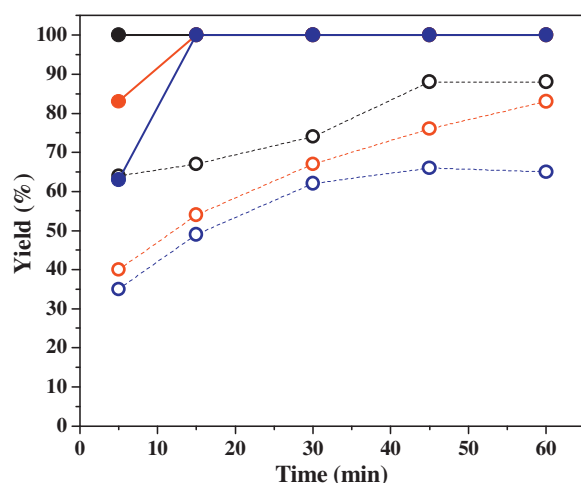
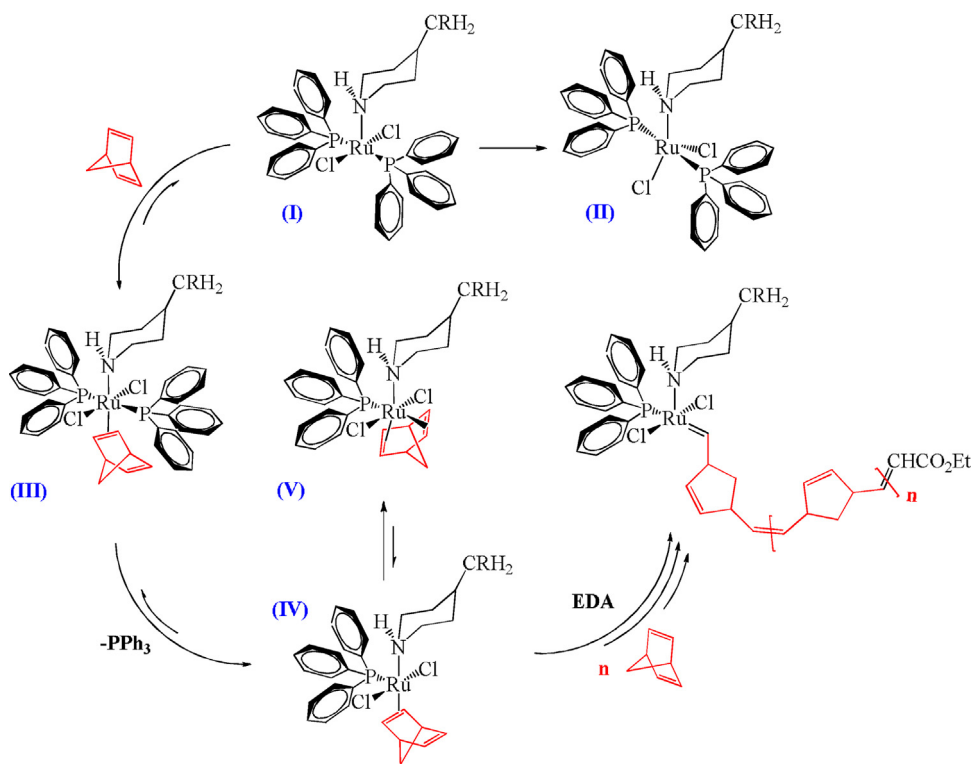


Fig. 3. Dependence of yield on the reaction time for ROMP of NBE with **1** (●), **2** (●), and **3** (●); [NBE]/[Ru] = 5000 with 1.1 μmol of the initiator in CHCl₃ at 25 °C (dash line) and 50 °C (solid line); 2 μL of EDA.



Scheme 1. Proposed mechanism for the geometrical rearrangement (**I** → **II**) and the reaction with NBD (**I** → **V**).

For runs at $[NBE]/[Ru] = 7000$ in 2 mL of solvent, the yields decreased using any initiator either at 25 or 50 °C (Fig. 4). This can be associated with the fast gelation of solution, affecting the propagation step. In experiments with **3** at $[NBE]/[Ru] = 7000$ in 10 mL, the gelation effect was minimized, resulting in 92% yield ($PDI = 2.8$; $M_w = 6.4 \times 10^4$ g mol $^{-1}$). For runs with molar ratio of 10,000 at 50 °C in the presence of **3**, the yield dropped to 76%, but with large M_w (1.3×10^5 g mol $^{-1}$; $PDI = 2.8$).

Experiments performed with excess of PPh_3 showed c.a. 18–32% yield at 50 °C for 30 min at $[NBE]/[Ru] = 5000$. In the presence of the respective amine, the yields were less than 2% of polyNBE under the same conditions. In the latter case, the amine probably coordinated into the SP vacant position of the starting complexes, preventing

ROMP initiation. With phosphine, the induction period was probably delayed, but ROMP occurred. Although the initiation and propagation reactions could also be affected, the major inhibitory process must be the release of PPh_3 in the induction periods, as earlier discussed with similar $[\text{RuCl}_2(\text{PPh}_3)(\text{amine})]$ complexes [19,20]. Thus, the polyNBE yield as a function of time at different temperatures can be explained (Fig. 3), where favorable conditions to release PPh_3 at 50 °C were established, resulting in better yields. Longer reaction time is then necessary for reaching high yields at 25 °C. In this context, a long induction period occurred at 25 °C, whereas a rapid production of the catalytic species at 50 °C provided better yields for short periods. Consequently, the induction period is critical to make use of these initiators for ROMP.

It is clear that the reaction time and monomer concentration improved the polymer yields. However, the reaction appeared to be more sensitive to temperature, where the yields were independent of the initiator type at 50 °C.

Fig. 5 shows correlation among the PDI values for different reaction times at $[NBE]/[Ru] = 5000$. In the case of **1**, except for 5 min, the PDI values did not show dependence neither on the reaction time nor temperature, contrary to the case of **2** where large variance was noted. Excluding the value for 15 min at 25 °C with **2**, the remaining values are equal; the same behavior is observed with **3**, where the values are roughly the same at 25 °C and enhance up to 0.3 units at 50 °C. The results with **3** are the lowest in the set, either at 25 or 50 °C.

The M_w values increased one order of magnitude (from 10^4 to 10^5 g.mol $^{-1}$) in each case when the experiments were carried out at 50 °C and $[NBE]/[Ru] = 5000$, with the tendency to decrease the PDI values, which were not time dependent, as already commented (Fig. 5). Considering the improvement in the yields at 50 °C for short periods, the results from M_w and PDI can support the fact that temperature provides short induction periods. The M_w values from the experiments as a function of $[NBE]/[Ru]$ molar ratio were within the same order of magnitude (10^4 g mol $^{-1}$), except for 5000 units at 50 °C (10^5 g mol $^{-1}$), with variation on the PDI values (Table S2).

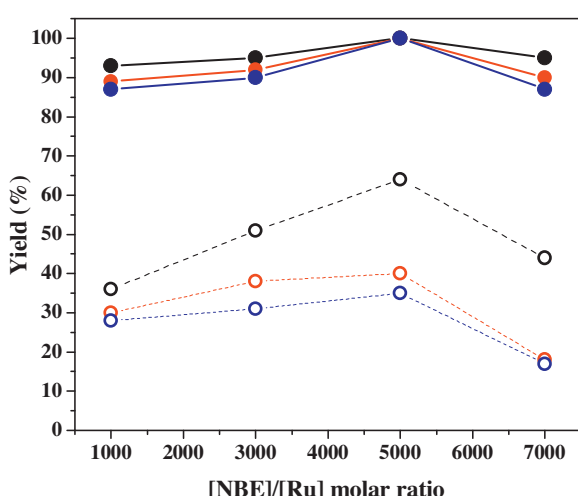


Fig. 4. Dependence of yield on the $[NBE]/[Ru]$ molar ratio for ROMP of NBE with **1** (●), **2** (○) and **3** (●); 1.1 μmol of initiator in CHCl_3 at 25 °C (dash line) for 5 min and 50 °C (solid line) for 30 min; 2 μL of EDA.

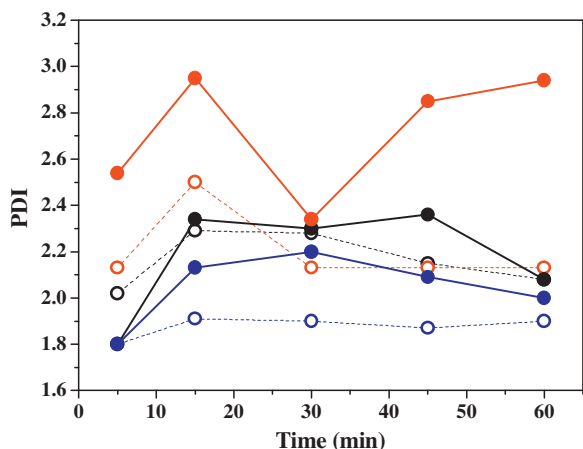


Fig. 5. Correlation among the PDI values for different reaction times for ROMP of NBE with **1** (●), **2** (●) and **3** (●); [NBE]/[Ru]=5000 with 1.1 μmol of initiator in CHCl₃ at 25 °C (dash line) and 50 °C (solid line); 2 μL of EDA.

Runs in air for 30 min at 50 °C and [NBE]/[Ru]=5000, resulted in yields in the range of 68–77% with **1**, **2** or **3**. Although this is a decrease of *c.a.* 30% in yield compared with the runs carried out in argon, these initiators presented reasonable reactivity in the presence of O₂ from the air.

It is worth mentioning that the catalytic activities of **1**, **2** and **3** for ROMP of NBE are comparable to other systems, where the Ru–carbene activity species were also generated *in situ* by diazo-compounds [29–32].

3.3. Synthesis of polymers from NBD

PolyNBD yields for different reaction times increased from *c.a.* 35% for 5 min to quantitative yields for 60 min at 25 °C with any initiator. At 50 °C, quantitative results were obtained after 30 min regardless of the initiator. Difference in the reactivity in the same order **1**>**2**>**3** can be verified either at 25 or 50 °C, as observed for ROMP of NBE (Fig. 6).

Quantitative consumption of NBD occurred at 25 °C for 60 min with all initiators at [NBD]/[Ru] molar ratios from 2000 to 5000 (Fig. 7). Difference in the yields in the order **1**>**2**>**3** for [NBD]/[Ru] molar ratios lower than 2000 can also be observed.

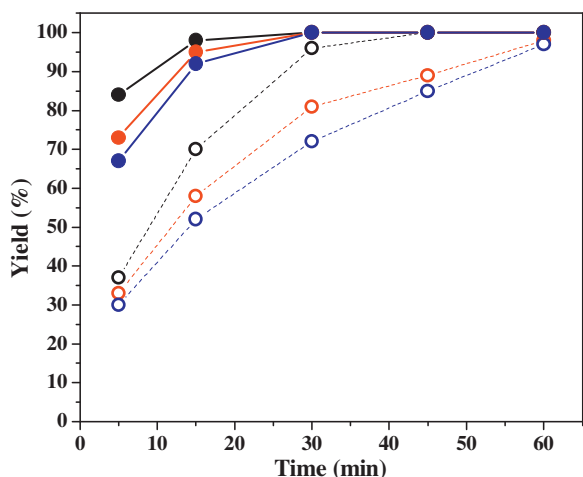


Fig. 6. Dependence of yield on the reaction time for ROMP of NBD with **1** (●), **2** (●), and **3** (●); [NBD]/[Ru]=5000 with 1.1 μmol of initiator in CHCl₃ at 25 °C (dash line) and 50 °C (solid line); 2 μL of EDA.

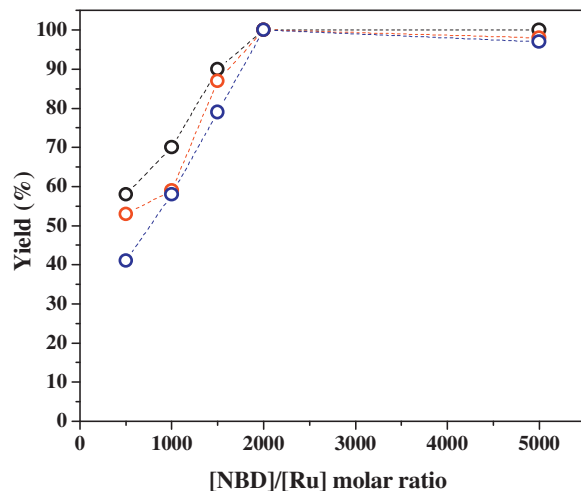


Fig. 7. Dependence of yield on the [NBD]/[Ru] molar ratio for ROMP of NBD with **1** (●), **2** (●), and **3** (●); 1.1 μmol of initiator in CHCl₃ at 25 °C for 60 min; 2 μL of EDA.

Quantitative yields were also obtained for reactions at molar ratios of 7000 and 10,000 when using complex **3** for 30 min at 50 °C.

The polyNBD were insoluble in CHCl₃ and molar weights were not obtained.

3.4. Concerning the relative catalytic activities of initiators

The yields for both polyNBE and polyNBD were dependent on the reaction time and starting [monomer]/[Ru] molar ratio with different trends in the curve profiles. At 25 °C, the curves for polyNBD show quantitative yields (Figs. 6 and 7), whereas the curves for polyNBE tend to present saturation profiles far from quantitative yields (Figs. 3 and 4). At 50 °C, quantitative results for both monomers are observed in spite of the different reaction times (15 min for polyNBE and 30 min for polyNBD). In particular, the yields for 5 min show a tendency to be lower for polyNBD than for polyNBE (Figs. 3 and 6).

An explanation for the different profiles is the occurrence of a double coordination of the NBD to the ruthenium metal center, which can lead to a sequence of reactions following ³¹P NMR analyses, as illustrated in the Scheme 1.

The ³¹P NMR spectra (Fig. S1) of the complexes in the presence of NBD showed new species in solution (Scheme 1), with the disappearance of signal at 62.7 ppm (species I) and the appearance of new singlet signals at –4.86, 22.4, 23.2, 29.8, and 32.9 ppm. It is reasonable to note the signal at 22.4 ppm to a six-coordinated species with NBD (species III), which loses a PPh₃ to produce a five-coordinated complex with signal at 23.2 ppm (species IV); this implies the presence of signals at –4.86 ppm for free PPh₃ and 29.8 ppm for OPPPh₃. The species IV is in equilibrium with a NBD-chelated six-coordinated isomer with signal at 32.9 ppm (species V).

The COSY-NMR spectra of the complexes obtained in the presence of NBD support the idea of a Ru–NBD double coordination. The spectra showed four groups of signals (Fig. S2), which were not observed neither in the spectrum of the complex, nor in the spectrum of the NBD, when they were evaluated separately. Signals at 5.12 and 4.73 ppm were assigned to the H^{2,3} and H^{5,6} olefinic protons, respectively, with the NBD as a chelating agent (Scheme 1, species V) [33–35]. In this case, the olefinic protons are not magnetically equivalent because the two double bonds are in different chemical environments. Signals at 4.48 and 4.10 ppm were attributed to the olefinic protons H^{2,3}, corresponding to the species IV and III, respectively, where the NBD is mono-coordinated. It was

possible to observe the coupling of the H^{2,3} and H^{5,6} with the H^{1,4} (3.82 ppm), confirming that these signals are related to the NBD.

The occurrence of competitive reactions can afford long induction period, resulting in low ROMP yields of polyNBD for short periods. However, quantitative monomer consumption was obtained when the reaction time was increased (Fig. 6). In addition, higher temperatures disfavor the double coordination and, consequently, quantitative yields were obtained at 50 °C.

When comparing the catalytic activity of complexes, even in the reactions with NBD, it is interesting to point out that **1** showed the highest results under the studied conditions, followed by **2** and **3**.

The unique difference in the complexes is the R substituent *para*-positioned in the piperidine ring, that is, –CH₂(H) in **1**, –CH₂(OH) in **2**, and –CH₂(Ph) in **3**.

Significant steric hindrance effect around the metal center from the substituent was not expected, as they were axially positioned (Fig. 1). This was supported by the fact that the R substituent size order (H < OH < Ph) does not correlate to the general yield results of ROMP (H > Ph > OH).

The other parameter to evaluate yield results should be associated with the electronic effects. The methyl group in **1** (R=H) is electron donor, whereas the benzyl in **2** (R=Ph) and the methanol groups in **3** (R=OH) behave as electron-withdrawing. Thus, the hydroxyl substituent in the case of **3** should afford the lowest piperidine σ-donation to activate the monomer via electronic synergism, with small tendency to produce polymer. Similar evaluation could be elaborated for **2**. On the other hand, enhanced yields should be expected in the case of **1** because of the contrary electronic effect. However, an electronic effect from the substituent to modulate the behavior of amine ligands through amine → Ru → monomer electronic synergism is contradictory to the very small difference in the expected pK_a values.

Apart from steric and electronic effects from 4-CH₂R-pip, a suggestion to understand the difference in the reactivity of the initiators is the occurrence of intra/intermolecular interactions. In the case of **3** (R=OH), an intermolecular Ru–O interaction between neighbor Ru complexes can block the vacancy positions in the Ru metal centers, increasing the induction period. The occurrence of Ru–O interactions in pure solutions hinders the geometrical rearrangement from SP to TBP (species **I** → **II**; Scheme 1), as well as the progress of ROMP when in the presence of monomer and EDA. This assumption is supported by the fact that the signals at 45.0 ppm in the ³¹P NMR spectra from complex **3** in pure solutions took relatively less time to appear than in the cases of complexes **1** and **2**.

In the case of complex **2** (R=Ph), weak intramolecular CH–π interactions can be formed between the CH of the Ph ring from

PPh₃ and the π-electronic ring from the Ph in 4-CH₂Ph-pip, (PPh₃)C–H···π/Ph(pip), as observed for other complexes [36,37]. These cooperative effects stabilize the five-coordinated adduct avoiding the release of the PPh₃ ligand from the Ru center. In this case, the rearrangements **I** → **II** (Scheme 1) were faster than with **3**; the relative time is in the following order: **1** > **2** > **3**.

The OH and the Ph interactions can explain the differences noted in the yield results. Whereas the electronic interactions in **2** and **3** provide low Ru activities, the CH₃ group in **1** is innocent, resulting in the reactivity order **1** > **2** > **3**. At 50 °C, however, these inter/intramolecular interactions tend to disappear, affording quantitative yields for both monomers because of the absence of Ru-deactivations from the piperidine R substituents.

3.5. Synthesis of copolymers from NBE and NBD

Four ROMCP batches were carried out mixing a fixed amount of NBE with four different amounts of NBD at RT for 60 min, in the presence of an initiator. The samples were labeled as [NBE]_n[NBD]_n, where the subscript numbers indicate the [monomer]/[Ru] molar ratio for each starting monomer. The n value (500, 1000, 1500 and 2000) represents the loading of NBD in the starting compositions.

The isolated materials were analyzed by ¹³C NMR spectroscopy and the signals in the spectra suggested the presence of M₁M₂ and M₂M₁ heterodyads, confirming the production of poly[NBE-co-NBD] copolymers (Fig. S3); the M₁ and M₂ representations denote the NBE and NBD mer-units, respectively. The spectra showed signals associated with the olefin (132–135 ppm) and methylene (32–49 ppm) carbons, following assignments early described (Table S3) [38,39].

The cis-double bond fractions (σ_c) were determined from the C^{1,4} and C^{1',4'} methylene carbon signals (Table 1). The σ_c values show similar stereo-selectivity in the copolymer samples for both NBE and NBD, with a slight tendency to trans stereo-selectivity for the NBE mer-units. The obtained results correlated well with the literature [38,39], where similar Ru-based catalysts usually do not produce selective synthesis of highly cis-polyNBEs. These initiators afforded a slight trans configuration of the carbon–carbon double bond and a blocky distribution of the double bond dyads [34,35]. Further, the microstructures of the resulting polymers were similar to the data previously reported for the copolymers prepared with the parent complexes [21,33].

The calculated reactivity ratios r_c (cc/ct) and r_t (tt/tc) of c.a. 0.8 and 1.4, respectively, with an $r_c \cdot r_t$ value of c.a. 1.2, suggest a blocky distribution, following the literature (σ_c values in the range of 0.35–0.85 with $r_c \cdot r_t > 1$ [1]). The $r_c \cdot r_t$ values for NBD units were

Table 1

Fraction of cis double bonds (σ_c), $r_c \cdot r_t$ and M₂/M₁ ratios determined from the ¹³C and ¹H NMR spectra of the copolymers obtained from different starting [NBE]₅₀₀₀[NBD]_n compositions.

Initiator	n value	$\sigma_c^{1,4}$		$\sigma_c^{1',4'}$		$r_c \cdot r_t$ (C ^{1,4})	M ₂ /M ₁ ratio	
		¹³ C	¹ H	¹³ C	¹ H		Found	Calcd.
1	500	0.44	0.45	0.44	0.45	1.18	0.08	0.10
	1000	0.44	0.44	0.58	0.56	1.22	0.11	0.20
	1500	0.45	0.45	0.49	0.50	1.29	0.18	0.30
	2000	0.45	0.46	0.50	0.50	1.24	0.23	0.40
2	500	0.44	0.46	0.51	0.52	1.13	0.05	0.10
	1000	0.44	0.46	0.57	0.56	1.33	0.12	0.20
	1500	0.45	0.44	0.58	0.58	1.30	0.14	0.30
	2000	0.46	0.47	0.59	0.60	1.20	0.16	0.40
3	500	0.44	0.45	0.51	0.50	1.27	0.05	0.10
	1000	0.44	0.44	0.52	0.53	1.25	0.10	0.20
	1500	0.46	0.45	0.60	0.58	1.21	0.15	0.30
	2000	0.45	0.46	0.56	0.55	1.24	0.19	0.40

M₂ = NBD; M₁ = NBE.

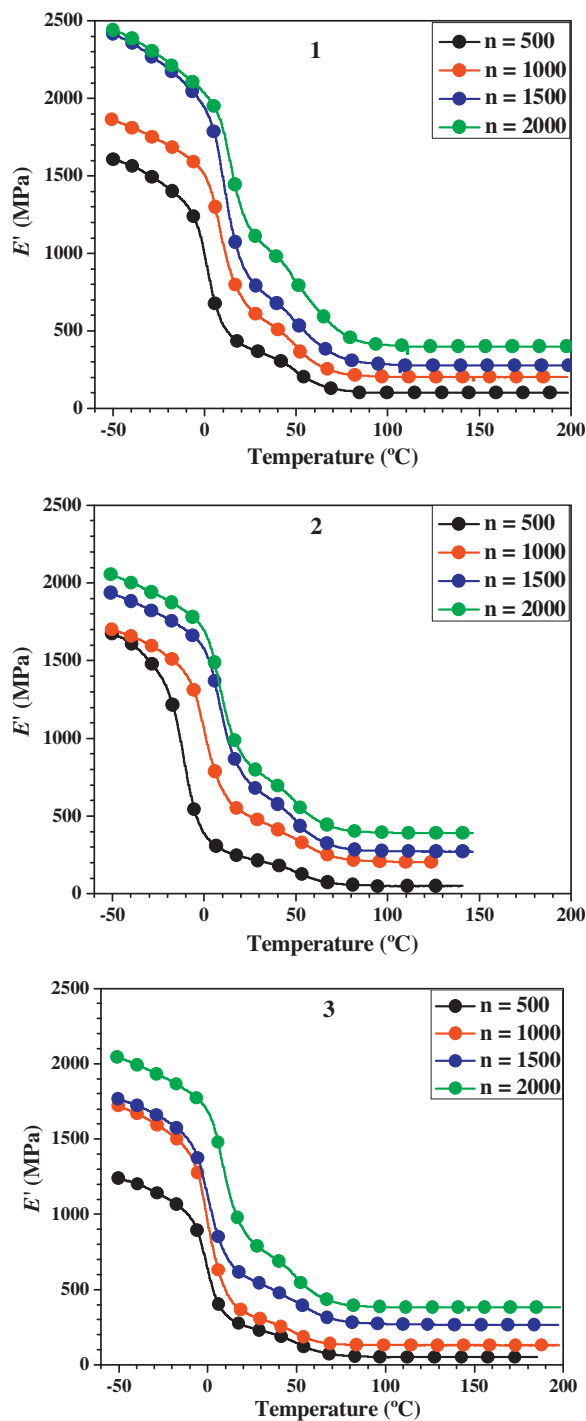


Fig. 8. Storage modulus curves for the copolymers obtained from different starting $[NBE]_{5000}[NBD]_n$ compositions with **1**, **2** and **3**.

not calculated because the signals for the M_2M_2 homodyads were not well split.

The σ_c values determined from the ^1H NMR spectra at 2.41 and 2.77 ppm ($\text{HC}^{1,4}$; *trans*- and *cis*-NBE units, respectively) and at 3.18 and 3.54 ppm ($\text{HC}^{1,4}$; *trans*- and *cis*-NBD units, respectively) were in agreement with those obtained from the ^{13}C NMR spectra (Table 1).

The M_2/M_1 ratios were also determined from the $\text{C}^{1,4}$ and $\text{C}^{1,4}$ methylene carbon signals, which correspond to the relative amount of NBD in the chains of the isolated copolymers. In general, the M_2/M_1 ratio increased when increasing the n value in the

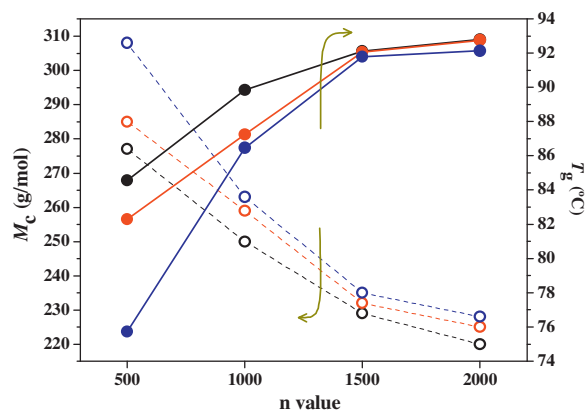


Fig. 9. Dependence of M_c (dash lines) and T_g (solid lines) on the n values for the copolymers obtained from different starting $[NBE]_{5000}[NBD]_n$ compositions with **1** (●), **2** (○), and **3** (●).

$[NBE]_{5000}[NBD]_n$ compositions (Table 1). The data also suggested that there is a slight tendency for more insertion of NBD when using **1**, whereas the results from **2** and **3** were roughly the same, considering the expected calculated values. The same profile was noticed for the production of homopolymers, where **1** showed a tendency to produce more polyNBE and polyNBD than the other two initiators.

The storage modulus (E') curves as a function of temperature indicated that all the copolymers were in the glassy state at the beginning of the measurements at -50°C (Fig. 8). In this region, the molecular chains were still restricted to molecular movements, where the thermal energy supplied was not enough to provide polymer chain movements [40–42]. When increasing the NBD content in the copolymers, the E' values in the glassy state also increased. Moreover, this characteristic was superior when **1** was used as initiator.

When the temperature was increased, the samples with more NBD tended to be less sensitive to the viscous component in each case (α relaxation), where the region of glass transition initiated at high temperatures compared with copolymers with low n values.

In the temperature range of *c.a.* 0 – 90°C , the storage modulus curves showed a drop of at least one order of magnitude related to the T_g for all samples. The T_g values were determined from the maxima of $\tan \delta$, which raised as the NBD amount in the isolated materials increased (Fig. 9).

After the α relaxation, the polymers reached the rubbery plateau with E' proportional to the amount of NBD monomers. This fact is an evidence for the existence of cross-linked networks in the copolymers, provided by second ring-opening from the NBD [21].

The molecular weights between the cross-linked chains (M_c) were determined from the rubbery modulus [40–42], decreasing as the NBD amount increased from 500 to 2000 (Fig. 9). As the M_c values decreased, the molecular motions become more restricted, decreasing the amount of energy that could be dissipated throughout the polymers [40–42]. This confirms that the increase of NBD in the copolymers resulted in more cross-linked networks, increasing the T_g and, consequently, enhancing the stiffness of materials.

The values from DMA analyses were also sensitive to the amount of NBD in the copolymers using any initiator. At low n values ($n = 500$ and 1000), a drastic increase in the T_g values was observed, while for higher n values ($n = 1500$ and 2000), the T_g values almost did not change. According to the catalytic activities for the homopolymers and copolymers, it is reasonable to affirm that initiator **1** provided the highest NBD insertion at low NBD contents. Nevertheless, when increasing the n values, the M_2/M_1 values presented saturation profiles for the three initiators, justifying similar T_g values with $n = 1500$ and 2000 .

4. Conclusion

The series of complexes of the type $[\text{RuCl}_2(\text{PPh}_3)_2(\text{amine})]$ was extended with three more amines, with the evidence that modifications on the attached groups in the cyclic amines affected the reactivity of the initiators for ROMP. Whereas the characteristics of the complexes were quite similar either in solid or solution states, homopolymer and copolymers with different characteristics were observed. It was proposed that the occurrence of intra/intermolecular electronic interactions involving the R substituents in **2** and **3** hindered the ROMP reactions. Initiator **1** was the most effective concerning the polymer yields and properties analyzed under different conditions for the ROMP of NBE and NBD and for the ROMCP of NBE/NBD.

Poly[NBE-co-NBD] were isolated with high degree of cross-linked chains, as judged from the M_c values and the high values of T_g , which were dependent on both NBD content and initiator type.

It is possible to conclude that alternative initiators with simple and cheap ancillary ligands can tune the reactivity of initiators for the ROMP and ROMCP of cyclic olefin, providing practical application toward preparative scale. This is an indicative of how a simple modification in usual complexes might affect polymer properties. Consequently, it is possible to design copolymers via olefin metathesis to reach desired properties for different applications.

Acknowledgements

The authors are grateful to FAPESP (Proc. 06/57577-4), CAPES, and CNPq for the financial support and to Dr. Debora T. Balogh for the DMA analyses performed at the Instituto de Física de São Paulo, São Carlos, SP, Brazil. The 400 MHz NMR analyses were performed at the Departamento de Química, Universidade Federal São Carlos, São Carlos, SP, Brazil.

Appendix A. Supplementary data

Supplementary material related to this article can be found, in the online version, at <http://dx.doi.org/10.1016/j.molcata.2014.01.012>.

References

- [1] K.J. Ivin, J.C. Mol, *Olefin Metathesis and Metathesis Polymerization*, Academic Press, New York, 1997.
- [2] R.H. Grubbs, *Handbook of Metathesis*, Wiley-VCH, Weinheim, 2003.
- [3] C.W. Bielawski, R.H. Grubbs, *Prog. Polym. Sci.* 32 (2007) 1–29.

- [4] A. Leitgeb, J. Wappel, C. Slugovc, *Polymer* 51 (2010) 2927–2946.
- [5] C.I. Mitan, V. Dragutan, I. Dragutan, *Rev. Roum. Chim.* 56 (2011) 299–316.
- [6] C. Samojlowicz, M. Bieniek, K. Grela, *Chem. Rev.* 109 (2009) 3708–3742.
- [7] J. Vougioukalakis, R.H. Grubbs, *Chem. Rev.* 110 (2010) 1746–1787.
- [8] D. Bek, R. Gawin, K. Grela, H. Balcar, *Catal. Commun.* 21 (2012) 42–45.
- [9] H. Clavier, K. Grela, A. Kirschning, M. Mauduit, S.P. Nolan, *Angew. Chem. Int. Ed.* 46 (2007) 6786–6801.
- [10] S. Mecking, A. Held, F.M. Bauers, *Angew. Chem. Int. Ed.* 41 (2002) 544–561.
- [11] A.M. Maj, L. Delaude, A. Demonceau, A.F. Noels, *J. Organomet. Chem.* 692 (2007) 3048–3056.
- [12] J.L. Pah, C.V. Bray, S. Dérien, P.H. Dixneuf, *J. Am. Chem. Soc.* 132 (2010) 7391–7739.
- [13] S. Camadanli, U. Decker, C. Kühn, I. Reinhardt, M.R. Buchmeiser, *Molecules* 16 (2011) 567–582.
- [14] S. Zhang, K. Nomura, *Catal. Surv. Asia* 15 (2011) 127–133.
- [15] J.M.E. Matos, B.S. Lima-Neto, *J. Mol. Catal. A: Chem.* 222 (2004) 81–85.
- [16] J.M.E. Matos, B.S. Lima-Neto, *Catal. Today* 282 (2005) 107–108.
- [17] J.M.E. Matos, B.S. Lima-Neto, *J. Mol. Catal. A: Chem.* 259 (2006) 286–291.
- [18] J.L. Silva Sá, B.S. Lima-Neto, *J. Mol. Catal. A: Chem.* 304 (2009) 187–190.
- [19] J.L. Silva Sá, B.S. Lima-Neto, *Appl. Catal.* 374 (2010) 194–200.
- [20] V.P. Carvalho Jr., C.P. Ferraz, B.S. Lima-Neto, *J. Mol. Catal. A: Chem.* 333 (2010) 46–53.
- [21] V.P. Carvalho Jr., C.P. Ferraz, B.S. Lima-Neto, *Eur. Polym. J.* 48 (2012) 341–349.
- [22] P.W. Armit, A.S.F. Boyd, T.A. Stephenson, *J. Chem. Soc., Dalton Trans.* (1975) 1663–1672.
- [23] P.R. Hoffman, K.G. Caulton, *J. Am. Chem. Soc.* 97 (1975) 4221–4228.
- [24] R.C.J. Vriend, G.V. Koten, K. Vrieze, *Inorg. Chim. Acta* 26 (1978) L29–L31.
- [25] K. Nakamoto, *Infrared and Raman Spectra of Inorganic and Coordination Compounds: Applications in Coordination, Organometallic, and Bioinorganic Chemistry*, John Wiley & Sons, Canada, 1997.
- [26] W. Baratta, A. Del Zotto, P. Rigo, *Organometallics* 18 (1999) 5091–5096.
- [27] F.M. Pedro, A.M. Santos, W. Baratta, F.E. Kühn, *Organometallics* 26 (2007) 302–309.
- [28] A. Demonceau, A.F. Noels, *J. Mol. Catal.* 76 (1992) 123–132.
- [29] E. Mothes, S. Sentets, M.A. Luquin, R. Mathieu, N. Lughan, G. Lavigne, *Organometallics* 27 (2008) 1193–1206.
- [30] M. Bernechea, N. Lughan, B. Gil, E. Lalinde, G. Lavigne, *Organometallics* 25 (2006) 684–692.
- [31] Y. Kong, Y. Tang, Z. Wang, S. Xu, H. Song, B. Wang, *Macromol. Chem. Phys.* 214 (2013) 492–498.
- [32] Y. Kong, Z. Wang, S. Xu, H. Song, B. Wang, *Organometallics* 31 (2012) 5527–5532.
- [33] J.L. Silva Sá, E.S.P. Nascimento, L.R. Fonseca, B.S. Lima-Neto, *J. Appl. Polym. Sci.* 127 (2013) 3578–3585.
- [34] T. Szymbańska-Buzar, T. Glowik, I. Czeluśniak, *Polyhedron* 21 (2002) 2505–2513.
- [35] T. Szymbańska-Buzar, T. Glowik, I. Czeluśniak, *J. Organomet. Chem.* 640 (2001) 72–78.
- [36] A. Malinowska, I. Czeluśniak, T. Szymbańska-Buzar, *J. Mol. Catal. A: Chem.* 26 (2005) 259–262.
- [37] C.A. Urbina-Blanco, A. Poater, T. Lebl, S. Manzini, A.M.Z. Slawin, L. Cavallo, S.P. Nolan, *J. Am. Chem. Soc.* 135 (2013) 7073–7079.
- [38] B. Bell, J.G. Hamilton, O.N.D. Mackey, J.J. Rooney, *J. Mol. Catal.* 77 (1992) 61–73.
- [39] I. Czeluśniak, T. Szymbańska-Buzar, *J. Mol. Catal. A: Chem.* 190 (2002) 131–143.
- [40] K.P. Menard, *Dynamic Mechanical Analysis: A Practical Introduction*, CRC Press, Boca Raton, 1999.
- [41] P.J. Flory, *Principles of Polymer Chemistry*, Cornell University Press, Ithaca, 1953.
- [42] G. Levita, S. DePetris, A. Marchetti, A. Lazzeri, *J. Mater. Sci.* 26 (1991) 2348–2352.